8-1-2011

Magnetic Properties of Monolayer Co Islands on Ir(111) Probed by Spin-Resolved Scanning Tunneling Microscopy

Jessica E. Bickel
Cleveland State University, j.e.bickel@csuohio.edu

Focko Meier
University of Hamburg

Jens Brede
University of Hamburg

André Kubetzka
University of Hamburg, kubetzka@physnet.uni-hamburg.de

Kirsten von Bergmann
Hamburg University, kbergman@physnet.uni-hamburg.de

See next page for additional authors

Magnetic properties of monolayer Co islands on Ir(111) probed by spin-resolved scanning tunneling microscopy

Jessica E. Bickel,* Focko Meier, Jens Brede, André Kubetzka, Kirsten von Bergmann, and Roland Wiesendanger
Institute of Applied Physics, University of Hamburg, Jungiusstrasse 11, D-20355 Hamburg, Germany
(Received 1 March 2011; revised manuscript received 16 May 2011; published 15 August 2011)

As the characteristic length scale of devices continues to decrease, it is essential to understand the fundamental magnetic properties of reduced dimension structures. This paper examines the electronic and magnetic properties of two-dimensional nanoscale Co islands on an Ir(111) surface using spin-polarized scanning tunneling microscopy. The pseudomorphic Co islands investigated are ferromagnetic and single domain, with the magnetic easy axis normal to the sample surface. Remarkably, the coercivity of these islands is greater than 4 T and magnetic saturation of the islands requires an applied field of at least 5 T.

DOI: 10.1103/PhysRevB.84.054454 PACS number(s): 75.75.−c, 68.37.Ef

I. INTRODUCTION

Material properties are intimately tied to both the amount of material present and the dimensionality of the structure. Thus it is important to understand how the fundamental properties of materials, such as magnetic structure, change as reduced dimension structures become more commonplace in devices. A significant reduction in device size was obtained in the field of magnetism by the discovery of the giant magnetoresistance (GMR),[1,2] which revolutionized the design of magnetic memory devices. The GMR requires two magnetic thin films, including one that is magnetically hard and does not change orientation in an applied field. Thus, in order to continue this size reduction, it remains critical to develop magnetically hard ferromagnetic nanostructures.

Magnetic nanostructures on atomically flat metal surfaces are an interesting model system to study fundamental magnetic properties in reduced dimensions. The 3*d* metals are of particular interest because of the demonstrated effect of reduced dimensions on magnetic properties such as anisotropy and coercivity[3,4] and magnetic ordering.[5] A complete description of magnetic properties in these systems relies on a comprehensive understanding of the structural properties, which have dramatic consequences for the spin-resolved electronic structure due to the influences of atomic orbital hybridization[6] and changes in magnetism due to reduced dimension effects.[4,5]

Cobalt films and nanostructures on noble metals have garnered much interest due to the experimentally measured and predicted high anisotropies and coercivities. Experimental studies of Co nanostructures on Pt show that both the magnitude and direction of the magnetic anisotropy depend critically on the structure of the Co as nanoislands or wires.[3,4,7] Theoretically, while Co monolayers and atoms on both Pt and Ir are predicted to have significant anisotropies and spin-orbit coupling,[8,9] it is predicted that the anisotropy of a Co monolayer on Ir will have a magnetic anisotropy ten times that of Co on Pt.[8] However, to the best of our knowledge, little work has been done to examine nanostructures of Co on Ir experimentally.

This paper investigates the magnetic structure of Co islands on the Ir(111) via spin-polarized scanning tunneling microscopy (SP-STM). Using this technique it is possible to resolve the electronic and magnetic structures on an atomic scale. The magnetic state, easy axis, and response to an external magnetic field of Co islands on Ir(111) are examined and characterized.

II. EXPERIMENTAL METHODS

Experiments were performed in two homebuilt UHV STMs with a base pressure of 10^{-11} mbar. The STMs were operated at cryogenic conditions of $T = 13$ and 6 K with out-of-plane (normal to the sample surface) magnetic fields of up to $B = 2.5$ and 6 T, respectively. All STM images were recorded in constant-current mode. The electronic and magnetic structure of the surface was probed by examining the differential conductance (dI/dU), which is closely related to the local density of states (LDOS) of the surface at a given energy eU.[10] The differential conductance was measured in two ways, each applying a small modulation to the applied bias voltage via a lock-in amplifier and then capturing the resulting dI/dU signal with the lock-in amplifier. The first method is scanning tunneling spectroscopy (STS), which was performed by stabilizing the tip at U_{stab} and I_{stab} and linearly ramping the voltage. Second, dI/dU slices were taken simultaneously with topography images at a single bias voltage of interest.

The Ir(111) substrate was prepared by sputtering, annealing to $T \approx 1300$ K for 5 min, and then cooling for 10–60 min. Cobalt was deposited by electron bombardment heating of a Co rod to evaporate material in a line of sight to the Ir surface. Samples were then transferred *in vacuo* to the STM.

The samples were examined with polycrystalline W tips that were etched *ex situ*, introduced to UHV, and then flashed *in vacuo* to remove any adsorbed impurities. Magnetically sensitive tips were created by depositing a thin Fe film ≈10–20 monolayers (ML) thick on the W tip and then annealing to form a smooth film. The magnetization direction of the Fe/W tip was controlled by applying a small magnetic field of $|B| = 300$–600 mT, which is sufficient to cant the tip magnetization such that it contains a significant out-of-plane component.

III. EXPERIMENTAL RESULTS

A. Sample morphology and electronic structure

Submonolayer amounts of Co grow pseudomorphically on Ir(111), as is seen in Fig. 1(a), despite a 7% lattice mismatch between film and substrate. The Ir(111) substrate exhibits

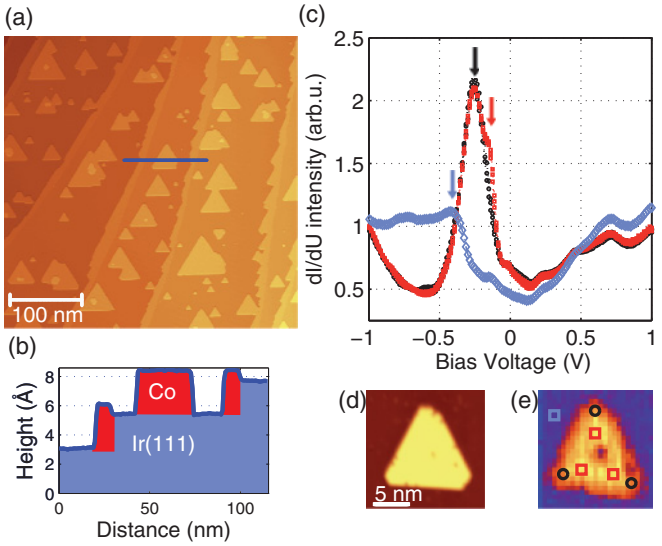

FIG. 1. (Color online) (a) STM topography image of Co islands and wires on Ir(111) and (b) corresponding height profile taken along the blue line in (a). (c) Spin-averaged dI/dU spectra of a typical Co/Ir(111) sample. This sample is shown below in (d), topography, and spectra were taken at the points marked in (e), a dI/dU slice of the same island. Arrows highlight the features of (left to right) the Ir, Co, and Co island center. All: W tip. (a), (b) $T = 6$ K, $B = -300$ mT, $U = -500$ mV, $I = 0.5$ nA. (c), (d), (e), $T = 13$ K. (c) $U_{\text{stab}} = +1.0$ V, $I_{\text{stab}} = 1.5$ nA. (d) $I = 1.5$ nA, $U = -400$ mV. (e) dI/dU slice taken at $U = -140$ mV.

monoatomic steps of height $h = 2.3 \pm 0.2$ Å [Fig. 1(b)] over the examined voltage range of $-1 \leqslant V \leqslant +1$ V, and the value is in agreement with the nominal value of $h = 2.22$ Å for bulk Ir. The deposited Co forms monolayer high triangular islands on the Ir terraces that vary significantly in size from $a = 10$ to 1300 nm^2 and sometimes show nucleation of a second layer of Co. Occasionally, dislocation networks are observed to relieve the strain between a Co island and the Ir substrate. The triangular shape of the Co islands is characteristic of growth on a close-packed surface such as the Ir(111). Two possible crystallographic stackings are possible on a close-packed surface. However, with very few exceptions, the triangular islands align in a single direction, indicating a single stacking for the Co.

In addition to forming islands, the deposited Co also attaches at the Ir step edges, forming Co wires of the same height as the Co islands, as seen in the height profile in Fig. 1(b). The edges of these Co wires are not smooth, but instead exhibit some faceting with the same low-energy edges as the triangular Co islands. The boundary between the Ir step edge and the Co wires shows no gap, as is clear in Fig. 1(b), and the wires coalesce with adjacent Co islands without formation of dislocations or height changes at the boundary. As Ir has fcc stacking, this indicates that the Co stacking is very likely also fcc with respect to the underlying Ir substrate.

The electronic structure of the Co islands is shown in Fig. 1(c). These spin-averaged dI/dU spectra were taken with a W tip on the single island shown in Figs. 1(d) and 1(e). Figure 1(d) shows the topography image of the island and Fig. 1(e) shows a dI/dU map which is taken as a constant voltage slice ($U = -140$ mV) of a full STS field. Spin-averaged dI/dU spectra were taken at the points marked in Fig. 1(e) and averaged to obtain the spectra in Fig. 1(c). The Ir substrate is rather featureless, with a step appearing at $U \approx -400$ mV, where $U = 0$ mV is the Fermi energy (E_{F}). This step, which is highlighted by the light blue (light grey) arrow in Fig. 1(c), is in agreement with previous measurements on Ir(111).[11,12] In contrast to the Ir substrate, the Co islands have a large peak at $U = -260$ mV, which is highlighted by the black arrow in 1(c). A small shoulder, which is highlighted by the red (dark grey) arrow in Fig. 1(c), appears at $U \approx -150$ mV for STS spectra taken in the center of the island (red squares) that disappears for spectra taken at the edge of the island (black circles). This can be seen clearly in the contrast of the dI/dU map in Fig. 1(e) taken at $U = -140$ mV. The black circles and red squares correspond to the markers in the STS spectra, and the dI/dU image highlights the edge of the island where the shoulder peak appears. (The depression at the center of the image is an impurity which can be seen on the topography image to the left-hand side.) Previous STS for Co/Cu(111),[13] Co/W(110),[14] and Co/Pt(111)[7] have also identified a Co peak at $U \approx -0.30$ eV. This peak appears to be characteristic of two-dimensional (2D) Co islands on these substrates, although the energy shifts slightly. It has been studied by a combination of photoemission and first-principle calculations[7,14–18] and interpreted as a d-like minority-surface resonance. This suggests that the peak seen for Co/Ir at $U = -260$ mV is also of d-like minority character.

B. Magnetic properties

The magnetic properties of the Co islands and wires were probed using a ferromagnetic Fe/W tip. Figures 2(a) and 2(b) show a topographic STM image and a simultaneously obtained dI/dU map of two Co islands taken at $B = +0.6$ T. Figure 2(c) shows a second dI/dU map of the Co islands imaged in an inverted magnetic field of $B = -0.6$ T. These dI/dU maps have a two-level contrast on the Co regions. As the contrast inverts concurrently with the magnetic field inversion, we can conclude it is magnetic (and not electronic) in origin. In fact, the contrast corresponds to the magnetic alignment of the islands parallel (red/light grey) and antiparallel (purple/dark grey) with respect to the out-of-plane component of the tip magnetization. When the applied field polarity is inverted, the alignment of the magnetic tip is inverted, as shown in inset of Fig. 2(d). This results in the inverted contrast of the islands seen in the dI/dU maps [Figs. 2(b) and 2(c)] because, while the tip magnetization direction changes, the magnetic direction of the Co islands does not change in these small magnetic fields. The single contrast level of each island coupled with the orientation of the Fe/W tip in the out-of-plane direction demonstrates that the Co islands are single domain ferromagnetic with an easy magnetization axis normal to the sample surface. This is in agreement with theory work that suggests an out-of-plane easy magnetization axis for Co atoms and ML films on Ir(111).[8]

The magnetic contrast can also be seen in STS spectra taken on the two islands at the points marked with an × in Fig. 2(a). The spectra shown in Fig. 2(d) were taken at $B = +0.6$ T (blue/dark grey) and $B = -0.6$ T (orange/light grey). As seen

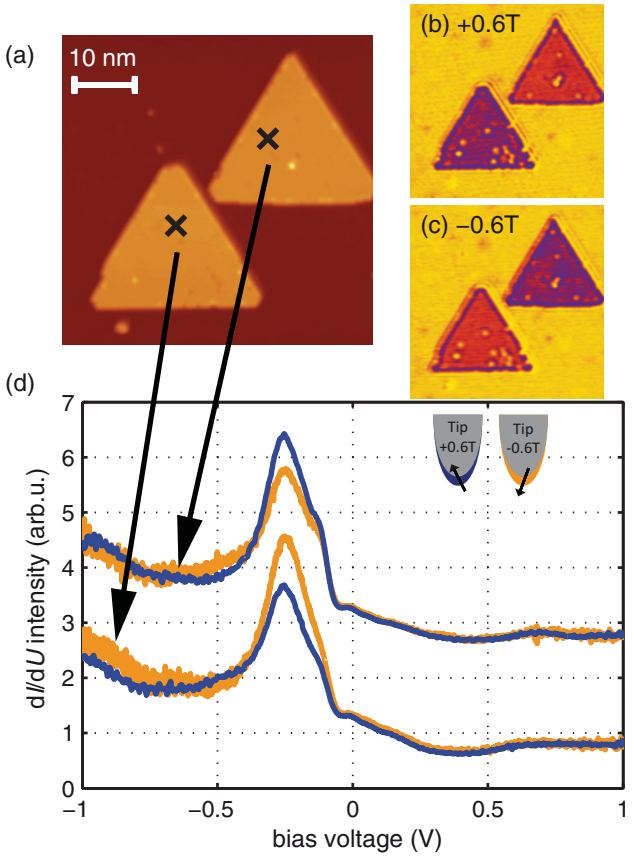

FIG. 2. (Color online) (a) Topography image of two Co islands, (b), (c) dI/dU maps taken at $B = \pm 0.6$ T, and (d) spin-resolved dI/dU spectra taken with an Fe/W tip at positions marked in (a). Upper spectra are off-set for clarity. Lower (upper) spectra belong to the left-hand (right-hand) island. All: $T = 6$ K. (a), (b), (c) $U = -250$ mV and $I = 2$ nA. (d) $U_{\text{stab}} = +1.0$ V, $I_{\text{stab}} = 1.5$ nA.

in the spectra, the presence of the characteristic −260 mV peak of the Co islands in the spin-averaged data is unchanged when examined with a spin-polarized STM tip. However, there is an intensity increase (decrease) of the peak on the left-hand (right-hand) island that reverses as the tip magnetization direction is inverted by inverting the applied magnetic field.

Few domain walls are present in the Co/Ir(111) sample. They occur only at constrictions in wires or at a coalescence point between two islands or an island and wire, and they form along the direction that minimizes wall length. One domain wall is shown in Fig. 3(a). The line profile taken perpendicular to this domain wall is shown in Fig. 3(b) along with a fitted profile. The fitting was made for a single 180° wall according to

$$y = y_0 + y_{\text{sp}} \tanh\left(\frac{x - x_0}{w/2}\right), \tag{1}$$

where y_0 and y_{sp} are the averaged and spin-polarized intensities, respectively, x_0 is the center of the domain wall, and w is the wall width. The extracted domain wall width is $w = 2.0$ nm with a fitting error of ±0.14 nm. The thickness of the Co wire at the point of the domain wall, i.e., the length of the domain wall, is 3 nm. When w is on the order of the domain wall length, these constrictions may in fact reduce

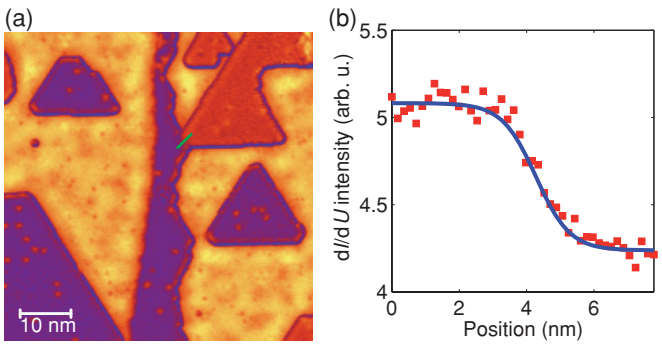

FIG. 3. (Color online) (a) Spin-resolved dI/dU image of a domain wall with the green line indicating the position of the height profile across the domain wall shown in (b) (red squares) and fitted (blue line) according to Eq. (1). Fe/W tip, $T = 13$ K, $U = -400$ mV, $I = 1.5$ nA, $B = +0.3$ T.

w. However, the infrequency of domain walls in this system makes fitting additional walls problematic.

The domain wall can be used to approximate the anisotropy of a system due to the inverse relationship between wall width and magnetic anisotropy, specifically:

$$w = 2\sqrt{\frac{A}{K_{\text{eff}}}}, \tag{2}$$

where A is the exchange stiffness and K_{eff} is the effective anisotropy constant. The exchange stiffness for a close-packed structure ML film can be estimated as $A_{\text{ML}} \approx \frac{3}{8} A_{\text{bulk}}$[19] to $\frac{1}{2} A_{\text{bulk}}$.[20] Using these values, the effective anisotropy can be calculated to be $0.78 \leqslant K_{\text{eff}} \leqslant 1.04$ meV/atom.[22] This is an upper limit of K_{eff} due to the domain wall fitting. However, increasing the domain wall width still results in a very high anisotropy, and the infrequency of domain walls on the surface also speaks to a high anisotropy.

This calculated K_{eff} is very high and is significantly higher than that of Co/Pt(111) (0.08–0.17 meV/atom[7]), which has been a model system for very high anisotropy nanostructures.[3,4,7,23,24] This high anisotropy is likely due to the interaction between the Co and the Ir surface. Co/Ir and Co/Pt both have high spin-orbit coupling (SOC), since SOC increases as the atomic number Z increases. Etz *et al.*[8] report a magnetocrystalline anisotropy (MAE) of ML Co on the Ir and Pt (111) surfaces of 1.395 and 0.123 meV/atom, respectively. Unfortunately, while the authors state that the orbital moments of monolayers are lower than for single atoms due to d-orbital filling differences and they state that orbital moment anisotropy is larger on Pt than Ir, the physical origin of the MAE differences for the complete monolayer of Co on Pt and Ir is not discussed. For comparison of this anisotropy value to the value reported in this work, it should be noted that this theory value from Etz *et al.* is the pure magnetocrystalline anisotropy whereas the K_{eff} determined here is an *effective* anisotropy which includes not only the MAE but also shape anisotropy which, though typically small for single ML systems,[8] will lower the measured anisotropy and edge atom effects which, due to a lower coordination number, may instead increase the measured anisotropy.

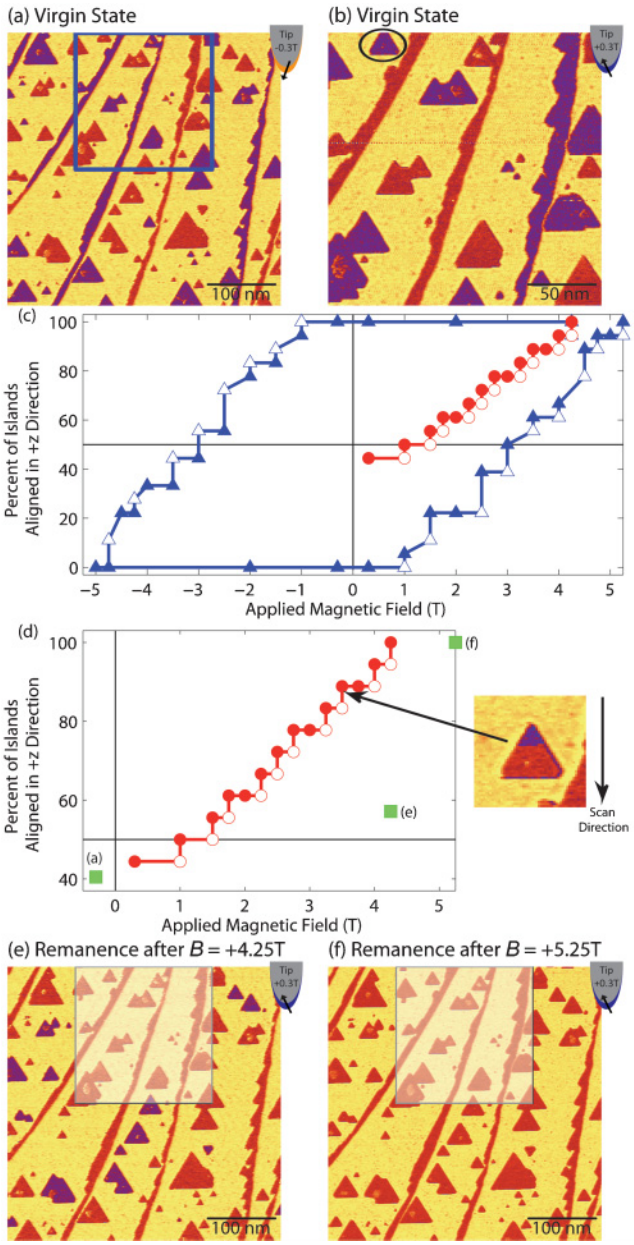

FIG. 4. (Color online) (a), (b), (e), (f) Spin-resolved dI/dU images. Note: (b) is a zoomed area from image (a) with opposite tip magnetization direction. (c) Hysteresis curve taken from the area shown in (b). The hysteresis curve starts from the virgin state (red circles) through a full magnetization demagnetization cycle (blue triangles). Open markers are the first image taken at applied field and closed markers are the final image taken at applied field. (d) Shows a zoom in of the virgin curve (red circles) and data points from the area *outside* the square region marked in (a), (e), and (f) (green squares). The inset of (d) shows an island [circled in (b)] undergoing a switching event. All: Fe/W tip, $T = 6$ K. (a), (b), (e), (f) $U = -500$ mV, $I = 0.5$ nA.

The high value determined for the anisotropy suggests that for Co islands on Ir(111) it will be difficult to switch the magnetization of the Co islands and the remanent magnetization and coercivity values will be high. These values were investigated by determining the hysteresis of the islands. Figure 4(a) shows a large-scale dI/dU image taken at $B = +300$ mT. Similar to Figs. 2(b) and 2(c), the magnetic contrast is confirmed by the contrast inversion of the islands upon reversal of the tip magnetization via a small applied external field. Figure 4(b) is a zoomed image of the region outlined in Fig. 4(a) with inverted tip polarity, and it can be seen that *all* the islands invert contrast between Figs. 4(a) and 4(b). This confirms that $|B| = 300$ mT is sufficient to align the tip magnetization such that it has a significant out-of-plane component but is insufficient to switch the magnetization direction of the Co islands.

Initially, as seen in the spin-polarized dI/dU images in Figs. 4(a) and 4(b) and in the virgin state in the hysteresis curve in Fig. 4(c), the surface has an almost equal distribution of islands aligned in the $+z$ and $-z$ directions, where the $+z$ ($-z$) direction is defined as aligned parallel (antiparallel) with a Fe/W tip in a positive polarity applied magnetic field. The area in Fig. 4(b) was repeatedly scanned while the magnetic field was increased in successive small intervals, resulting in the hysteresis curve shown in Fig. 4(c) where the percentage of islands aligned in the $+z$ direction is plotted versus the applied magnetic field. There appears to be a slight size dependence with higher magnetic fields required to switch the smaller islands, but this dependence is very small relative to the large scatter of area versus switching field. Regardless, the islands show complete remanence, as is seen by the 100% alignment as the applied field is reduced and inverted ($B = 0$ T), and a coercive field of $H_c \approx 3$ T is measured. This is a very high value relative to common coercivities such as $H_c \approx 1$–1.5 T for Co/Cu(111)[25] or $H_c = 0.25$ or >2.0 T for monolayer and double-layer Co islands on Pt(111),[7] which is in agreement with the high values measured here for the anisotropy of Co/Ir(111) relative to these other systems. A very large saturation field of $B = +5.25$ T was required to align all the islands in the $+z$ direction.

Two items must be further discussed with regard to the hysteresis curve in Fig. 4(c). The first is the discrepancy between the saturation field required to align the virgin magnetic state, $H_c = +4.25$ T, and that to complete the hysteresis curve, $H_c = +5.25$ T. The second is the stairstep shape of the hysteresis curve. Both of these points are explained by the occurrence of tip-induced switching of the islands. An enlarged version of the virgin curve is shown in Fig. 4(d). As for the full hysteresis curve in Fig. 4(c), the virgin curve has two types of markers. The open markers correspond to the first image taken at the applied field and the closed markers correspond to the final image taken at the applied field. Multiple images were taken at each applied magnetic field due to the observation of switching events that occurred during scanning, such as the one shown in Fig. 4(d). It should be noted that islands can only switch to a direction parallel to the applied external field and tip magnetization, as is the case here where the contrast changes from antiparallel (purple/dark grey) to parallel (red/light grey). This island was scanned from top to bottom, and it can be seen that the island contrast changes $\approx 1/3$ of the way through the island. It is clear this is a switching event because the contrast change is perfectly horizontal, perpendicular to the slow scan direction, and a scan taken immediately following such an event shows a completely aligned island. Such switching events occurred over the entire range of applied magnetic fields and could account for up to a 16% change in the percent of islands aligned in the $+z$ direction, as seen in the hysteresis

curve in Fig. 4(c). The reason for these switching events is the magnetic stray field of the Fe/W tip. Previous work has shown that a Fe/W tip exhibits a stray field, which may influence domain wall movement and switching field.[26] Since the tip magnetization contains a significant component that is parallel to the external applied field, its stray field increases the applied field acting on the magnetic islands. The tip magnetization may also contribute to switching events by adding an in-plane component to the applied magnetic field, which may reduce the energy barrier for island switching. These switching events explain not only the change as a function of number of scans in the percentage of islands aligned in the $+z$ direction, but also the irreproducibility in the measured saturation magnetization. This is because the percent of islands aligned in the $+z$ direction is dependent on *both* the applied field and the number of times the islands are scanned. This means that the alignment of the islands, and as such the measured saturation field and coercivity, depend on the number of scans taken at each applied magnetic field as well as the number of magnetic intervals examined.

Tip-induced switching is a local process which only acts on islands in a close vicinity to the STM tip and so would only affect the area that was repeatedly scanned to determine the hysteresis loop shown in Fig. 4(b) and highlighted with squares in Figs. 4(a), 4(e), and 4(f), which we will hereafter call region ⋆. Thus, in order to better understand the influence of this process on the measured magnetic properties, we investigated an area adjacent to region ⋆. Figure 4(e) shows the same region examined in Fig. 4(a) measured in remanence after an applied field of $B = +4.25$ T. The area highlighted by the square was scanned under applied fields of up to $B = +4.25$ T in order to determine the virgin curve as previously described. The field was then reduced to $B = +0.3$ T and a large scale image was taken, which is shown in Fig. 4(e). Figure 4(f) was obtained by the same method after an applied field of $B = +5.25$ T. As shown before, this small applied field of $|B| = 0.3$ T is sufficient to align the magnetic tip in the field direction but insufficient to change the Co island magnetization direction. As the islands exhibit a 100% remanence, as is shown in the hysteresis loop, this is an ideal way to examine the results of an applied field without tip-induced stray-field effects. As can be seen in Fig. 4(e), after an applied field of $B = +4.25$ T, the area *outside* region ⋆ exhibits few switched islands relative to its virgin state shown in Fig. 4(a), while the area *inside* region ⋆ is completely aligned. An applied field of $B = +5.25$ T [Fig. 4(f)] is required to fully align the islands outside the scanned area.

The values obtained by examining the remanence magnetization images in Figs. 4(e) and 4(f) are plotted with the virgin curve in Fig. 4(d) as green squares. These data points suggest the coercivity is higher than the $H_c = 3$ T found in the full hysteresis loop. The values reported reflect only the area *outside* region ⋆ as is highlighted in each of the images, Figs. 4(a), 4(e), and 4(f). Note there is a slight difference in the values taken from Figs. 4(a) and 4(b) due to the different image size altering the number of islands examined. The discrepancy seen visually in Fig. 4(e) between the alignment of islands *inside* versus *outside* region ⋆ is clearly seen in Fig. 4(d) by comparing the final point on the virgin curve where the islands are 100% aligned with the applied magnetic field and

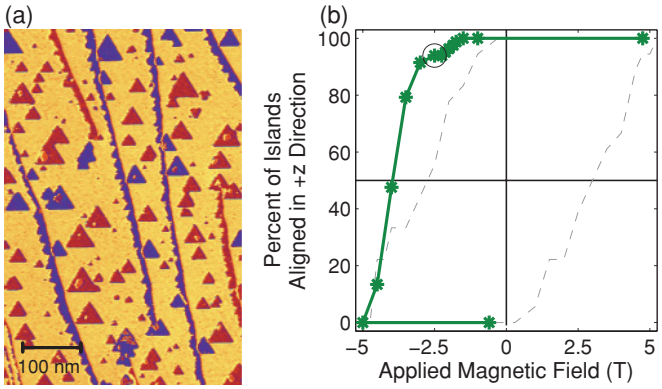

FIG. 5. (Color online) (a) Spin-resolved dI/dU image taken at $B = -2.5$ T and (b) hysteresis curve corresponding to the area shown in (a). The gray dashed line is the hysteresis loop from Fig. 4(b) shown for reference. The circle in (b) indicates the applied magnetic field of (a). Fe/W tip, $T = 6$ K, $U_{\text{bias}} = -500$ mV, $I = 0.5$ nA.

the point marked (e) where the islands show less than 60% alignment with the external magnetic field. Applying a field of $B = +5.25$ T, however, is enough to fully align the islands both inside and outside region ⋆ as is seen for the point (f) and Fig. 4(f). This suggests that the measured coercivity of the Co islands in Fig. 4(c) of $H_c = 3$ T is a *minimum* estimate as the stray-field-induced switching results in lower required applied fields to align the Co islands.

This influence of stray-field switching is confirmed by a second measurement on the same sample after the Fe/W tip apex underwent a change, resulting in the possibility of a different stray field and magnetic orientation, including a different possible in-plane component. The second loop, shown in Fig. 5(b), was taken over a larger area ($\approx 400 \times 600$ nm^2), as can be seen in Fig. 5(a), and taking only a single image at each magnetic field. Islands at the image edge and islands touching Co wires were excluded from the analysis. The results of this loop show very little switching of the islands up to $|B| = 3$ T (94% aligned) and a higher measured coercivity of $H_c = 4$ T, but the saturation field is identical to that shown in Fig. 4(c). These results indicate that the shape of the tunneling microtip and the magnitude of the resulting stray field it produces may *significantly* shrink the measured hysteresis loop.

The measured coercive field can also be used to estimate the effective anisotropy through the Stoner-Wohlfarth model for single-domain particles, which gives the relationship

$$M_s B_c = 2K_{\text{eff}}, \tag{3}$$

where B_c is the critical applied magnetic field, and M_s is the saturation magnetization. If B_c is taken to be the 4 T coercive field and M_s of a single atom is taken to be $1.9\mu_B$,[8] then $K_{\text{eff}} = 0.22$ meV/atom. For clarity in the following discussion, let K_{dw} and K_{SW} refer to the values of K_{eff} determined from the domain wall analysis and the Stoner-Wohlfarth analysis, respectively. K_{SW} is significantly smaller than K_{dw}, and this discrepancy can be explained in a few ways. The measured $H_c \approx 4$ T is a *lower limit* of the coercivity, meaning that K_{SW} is also a lower limit, while K_{dw} is an upper limit. Also, while there are no defects near the domain wall [Fig. 3(a)], K_{SW} is

determined by an average over many islands, some of which exhibit defects or nucleation of a second layer of Co which may alter the energy required to change the magnetization direction of an island. The islands were examined and no such correlation between switching field and the presence of defects was determined; however, the statistics of the analysis are low. Thus, through this analysis the actual value of the anisotropy is determined to be $0.22 \leqslant K_{\text{eff}} \leqslant 1.04$ meV/atom. The lower bound is still greater than that reported for Co/Pt(111),[7] which has been a model system for high anisotropy.

IV. CONCLUSIONS

We have examined Co islands grown on Ir(111). The Co grows pseudomorphically on the Ir(111) surface, exhibiting a predominately single stacking which is most likely fcc. The electronic structure of the islands exhibits a strongly spin-polarized peak at $U = -260$ mV. The spin-polarized contrast shows up clearly in spin-resolved dI/dU maps, demonstrating that the investigated islands are single domain ferromagnetic with the easy magnetization axis normal to the surface. The measured 4 T coercivity of these Co islands, extracted from hysteresis loops, is a lower limit due to the evidence of tip-stray-field-induced switching of the islands. The saturation field required to align all islands in the easy axis is $B = +5.25$ T. This high value for saturation, coupled with 100% remanence and high coercivity, means these islands are very stable under applied magnetic fields of a few tesla. This makes Co/Ir(111) an ideal template for spin-polarized inversion studies where it is important to be able to invert the tip magnetization without altering the surface magnetization.

ACKNOWLEDGMENTS

We would like to thank S. Krause and R. Wieser for valuable discussions and C. Hanneken for experimental insight. Financial support from the Alexander von Humboldt Foundation, the DFG via SFB668-A8, the ERC Advanced Grant FURORE, and the Hamburgische Stiftung für Wissenschaft und Forschung (Cluster of Excellence NANOSPINTRONICS) is gratefully acknowledged.

*jbickel@physnet.uni-hamburg.de

[1] G. Binasch, P. Grünberg, F. Saurenbach, and W. Zinn, Phys. Rev. B **39**, 4828 (1989).

[2] M. N. Baibich, J. M. Broto, A. Fert, F. Nguyen Van Dau, F. Petroff, P. Etienne, G. Creuzet, A. Friederich, and J. Chazelas, Phys. Rev. Lett. **61**, 2472 (1988).

[3] P. Gambardella, S. Rusponi, M. Veronese, S. Dhesi, C. Grazioli, A. Dallmeyer, I. Cabria, R. Zeller, P. Dederichs, K. Kern *et al.*, Science **300**, 1130 (2003).

[4] S. Rusponi, T. Cren, N. Weiss, M. Epple, P. Buluschek, L. Claude, and H. Brune, Nat. Mater. **2**, 546 (2003).

[5] A. Bala and T. Nautiyal, J. Magn. Magn. Mater. **320**, 2201 (2008).

[6] H. J. Gotsis, N. Kioussis, and D. A. Papaconstantopoulos, Phys. Rev. B **73**, 014436 (2006).

[7] F. Meier, K. von Bergmann, P. Ferriani, J. Wiebe, M. Bode, K. Hashimoto, S. Heinze, and R. Wiesendanger, Phys. Rev. B **74**, 195411 (2006).

[8] C. Etz, J. Zabloudil, P. Weinberger, and E. Y. Vedmedenko, Phys. Rev. B **77**, 184425 (2008).

[9] A. B. Shick and A. I. Lichtenstein, J. Phys. Condens. Matter **20**, 015002 (2008).

[10] J. Tersoff and D. R. Hamann, Phys. Rev. Lett. **50**, 1998 (1983).

[11] F. Marczinowski, K. von Bergmann, M. Bode, and R. Wiesendanger, Surf. Sci. **600**, 1034 (2006).

[12] J. F. van der Veen, F. J. Himpsel, and D. E. Eastman, Phys. Rev. B **22**, 4226 (1980).

[13] O. Pietzsch, A. Kubetzka, M. Bode, and R. Wiesendanger, Phys. Rev. Lett. **92**, 057202 (2004).

[14] J. Wiebe, L. Sacharow, A. Wachowiak, G. Bihlmayer, S. Heinze, S. Blügel, M. Morgenstern, and R. Wiesendanger, Phys. Rev. B **70**, 035404 (2004).

[15] L. Diekhöner, M. A. Schneider, A. N. Baranov, V. S. Stepanyuk, P. Bruno, and K. Kern, Phys. Rev. Lett. **90**, 236801 (2003).

[16] F. J. Himpsel and D. E. Eastman, Phys. Rev. B **20**, 3217 (1979).

[17] H. Knoppe and E. Bauer, Phys. Rev. B **48**, 1794 (1993).

[18] S. N. Okuno, T. Kishi, and K. Tanaka, Phys. Rev. Lett. **88**, 066803 (2002).

[19] $A \propto N$, where N is the coordination number of the atom. N is reduced from 12 for bulk to 6 for monolayer Co because Ir is nonmagnetic and so the three Ir neighbors can be ignored. As $A_{\text{bulk}} = 3.0 \times 10^{-11}$ J/m, this results in $A_{\text{ML}} = 1.5 \times 10^{-11}$ J/m.

[20] This estimation follows the derivation by Chikazumi,[21] which examines the exchange energy stored in a pair of spins $\vec{S}_i$ and $\vec{S}_j$. In this case, it can be shown that the exchange stiffness is proportional to the summation over the exchange energy of all such nearest-neighbor pairs. By examining this relationship in the context of the fcc(111) surface instead of the bulk crystal, it can be shown that $A_{\text{ML}} = \frac{3}{8} A_{\text{bulk}}$. Thus, this gives a value of $A_{\text{ML}} = 1.125 \times 10^{-11}$ J/m.

[21] S. Chikazumi, *Physics of Ferromagnetism* (Oxford University Press, Oxford, UK, 2002).

[22] It should be noted that the bulk atomic density of Co was used to report these values in terms of meV/atom in order to compare with other reported values.

[23] P. Gambardella, A. Dallmeyer, K. Maiti, M. C. Malagoli, W. Eberhardt, K. Kern, and C. Carbone, Nature (London) **416**, 301 (2002).

[24] P. Gambardella, A. Dallmeyer, K. Maiti, M. C. Malagoli, S. Rusponi, P. Ohresser, W. Eberhardt, C. Carbone, and K. Kern, Phys. Rev. Lett. **93**, 077203 (2004).

[25] O. Pietzsch, S. Okatov, A. Kubetzka, M. Bode, S. Heinze, A. Lichtenstein, and R. Wiesendanger, Phys. Rev. Lett. **96**, 237203 (2006).

[26] A. Kubetzka, M. Bode, O. Pietzsch, and R. Wiesendanger, Phys. Rev. Lett. **88**, 057201 (2002).